

TITLE: Rising Step Load Testing of AA7085-T7452

INVESTIGATOR: Associate Professor Michelle Gaudett Koul  
Department of Mechanical Engineering

BACKGROUND: The phenomena of environmentally assisted cracking (EAC) can be described as stable, subcritical crack growth that occurs at stress intensities below the fracture toughness of a material due to the combined actions of stress and corrosion. Much as the same way fatigue performance is considered in the presence of alternating loads, a material's susceptibility to EAC must be considered in material selection when the possibility of corrosion exists. EAC performance can be evaluated in terms of crack initiation resistance using smooth specimen testing, resulting in limiting loads as a function of failure time. This information can be used much in the same way S-N curves are used in to design against fatigue. However, the subject of this study involves test methods that support the damage tolerance approach to lifetime prediction, and utilize pre-cracked specimens. As in fatigue crack growth testing, the threshold stress intensity at which EAC initiates from a sharp crack can be measured ( $K_{th}$ ). In addition, the rate of environmentally assisted crack growth ( $V$ ) as a function of applied stress intensity ( $K$ ), can be obtained and are often referred to as V-K curves. These are analogous to the crack growth rate ( $da/dN$ ) versus applied stress intensity range ( $\Delta K$ ) curves observed in the fatigue literature.

As new and corrosion resistant alloys and alloy conditions become available, there is a need for testing procedures that clearly characterize and compare EAC performance. Due to the simplicity and low cost of crack initiation type testing, alloy manufacturers primarily provide data of this type. However it is not clear that EAC crack initiation performance for smooth specimens is a reliable indicator of material performance where the possibility of sharp defects exists. In addition, a high resistance to crack initiation does not necessarily imply slow propagation rates once EAC has initiated. Although a number of test techniques have been standardized, further clarifications are required as new alloys and new alloy conditions are evaluated that may possess different underlying EAC mechanisms compared to the alloy used to develop the standardized test.

#### METHOD AND RESULTS:

Tests were performed on (3) AA7085-T7452 specimens in the ST orientation. Specimen 62A was tested at constant crosshead displacement rate of 0.01 in/min in air. Specimen 62B was tested using a rising step load protocol of 400 lb load increments followed by 16h holds in ASTM D1141 artificial seawater. A modified RSL test was performed for specimen 62C in ASTM D1141 artificial seawater. Specimen 62C was loaded to an initial value of 2400 lbs ( $K = 17 \text{ ksi}\sqrt{\text{in}}$ ) followed by alternating holds of 42h and load increases of 400 lbs. This test protocol was chosen to explore the stress intensity range for which crack initiation was suspected in the previous test (62B), but allowing for longer exposure time. The hold time was chosen to keep testing within a week's time.

Tests were performed on (2) AA7085-T7452 specimens in the LT orientation. Specimen 63A was tested at constant crosshead displacement rate of 0.01 in/min in air. Specimen 63B was tested using a modified RSL test in ASTM D1141 artificial seawater. Specimen 63B was loaded to an initial value of 2400 lbs ( $K = 17 \text{ ksi}\sqrt{\text{in}}$ ) followed by alternating holds of 42h and load increases of 400 lbs.

Crack length as a function of time was calculated from COD gage measurements using equations developed by Saxena and Hudak for WOL specimens and were used to help detect subcritical crack initiation. An effective B that accounts for the side grooves was used. No attempt to calibrate these crack lengths based on actual measurement has been made.

Report Documentation Page				Form Approved OMB No. 0704-0188	
Public reporting burden for the collection of information is estimated to average 1 hour per response, including the time for reviewing instructions, searching existing data sources, gathering and maintaining the data needed, and completing and reviewing the collection of information. Send comments regarding this burden estimate or any other aspect of this collection of information, including suggestions for reducing this burden, to Washington Headquarters Services, Directorate for Information Operations and Reports, 1215 Jefferson Davis Highway, Suite 1204, Arlington VA 22202-4302. Respondents should be aware that notwithstanding any other provision of law, no person shall be subject to a penalty for failing to comply with a collection of information if it does not display a currently valid OMB control number.					
1. REPORT DATE <b>2007</b>		2. REPORT TYPE		3. DATES COVERED <b>00-00-2007 to 00-00-2007</b>	
4. TITLE AND SUBTITLE <b>Rising Step Load Testing of AA7085-T7452</b>				5a. CONTRACT NUMBER	
				5b. GRANT NUMBER	
				5c. PROGRAM ELEMENT NUMBER	
6. AUTHOR(S)				5d. PROJECT NUMBER	
				5e. TASK NUMBER	
				5f. WORK UNIT NUMBER	
7. PERFORMING ORGANIZATION NAME(S) AND ADDRESS(ES) <b>United States Naval Academy (USNA), Department of Mechanical Engineering, Annapolis, MD, 21402</b>				8. PERFORMING ORGANIZATION REPORT NUMBER	
9. SPONSORING/MONITORING AGENCY NAME(S) AND ADDRESS(ES)				10. SPONSOR/MONITOR'S ACRONYM(S)	
				11. SPONSOR/MONITOR'S REPORT NUMBER(S)	
12. DISTRIBUTION/AVAILABILITY STATEMENT <b>Approved for public release; distribution unlimited</b>					
13. SUPPLEMENTARY NOTES					
14. ABSTRACT					
15. SUBJECT TERMS					
16. SECURITY CLASSIFICATION OF:			17. LIMITATION OF ABSTRACT <b>Same as Report (SAR)</b>	18. NUMBER OF PAGES <b>8</b>	19a. NAME OF RESPONSIBLE PERSON
a. REPORT <b>unclassified</b>	b. ABSTRACT <b>unclassified</b>	c. THIS PAGE <b>unclassified</b>			

## Results

Crack initiation in air testing under monotonically increasing displacement is clear and is indicated by a distinct load drop and a large increase in crack length (Figure 1). Stress intensity values were calculated using equations in ASTM E1820-96 Section A2 and the measured pre-crack lengths shown in Table 1. The measured fracture toughness in air ( $K_q$ ) for the ST orientation (62A) is 27.9 ksi $\sqrt{\text{in}}$  and for the LT orientation (63A) is 41.2 ksi $\sqrt{\text{in}}$ .

Table 1 – Measured pre-crack lengths. (Assumed notch depth from load line to be 0.9-in.)

	Average fatigue pre-crack length (in)	Standard deviation (in)
62A	1.020	0.036
62B	0.982	0.027
62C	0.961	0.016
63A	1.024	0.044
63B	0.997	0.034

Crack initiation in the seawater test is less obvious. For specimen 62B, it is clear that fast fracture occurred at 3711 lbs ( $K_q = 26.8$  ksi $\sqrt{\text{in}}$ ) during an attempted step increase in the load from 3600 to 4000 lbs (Figure 2). However, the crack length vs. time data indicates a consistently positive slope at the last three load steps of 2800, 3200 and 3600 lbs that correspond to crack growth rates of  $\sim 1.5 \times 10^{-4}$  in/hr. This rate is consistent with measured Stage II crack growth rates in NaCl solutions for 7000 series alloys.

It has been observed that load relaxation effects at stress intensity values approaching the fracture toughness can result in artificial indications of crack growth. Therefore, SEM validation of the presence/absence of subcritical crack growth is required. Figures 3 and 4 show scanning electron micrographs of the fracture surfaces at the tips of the fatigue pre-cracks for 62A and 62B, respectively. The transition from fatigue to fast fracture is more difficult to discern in the seawater test due to corrosion damage. However, a less ductile fracture morphology (compared to the air test) is noted near the pre-crack tip, whose  $\sim 200$   $\mu\text{m}$  extent agrees with the small amount of subcritical crack growth expected (assuming subcritical crack initiation is indicated in the test data). In addition, a significant amount of corrosion product was noted on the fracture surface within 500  $\mu\text{m}$  of the pre-crack tip, perhaps indicating exposure to the test solution prior to fast fracture. Based on this information it is conservative to assume subcritical crack growth did occur at  $P = 2800$  lbs, and  $K_{EAC} = 20.2$  ksi $\sqrt{\text{in}}$  for specimen 62B.

Figure 5 shows the results for specimen 62C. Fast fracture occurred at 3721 lbs ( $K_q = 26.1$  ksi $\sqrt{\text{in}}$ ) during an attempted step increase in the load from 3600 to 4000 lbs. However, the crack length vs. time data indicates a consistently positive slope at the last load step of 3600 lbs that corresponds to a crack growth rate of  $1.9 \times 10^{-4}$  in/hr and a  $K_{EAC}$  of 25.2 ksi $\sqrt{\text{in}}$ . Figure 6 shows SEM micrographs of the fracture surface, with indications of an environmentally-affected fracture surface in the vicinity of the precrack. Figure 7 shows additional micrographs comparing an area in the environmentally-affected region to an area well away from the crack tip where fast fracture had occurred. The environmentally-affect region shows failure with significant plasticity, however, it lacks the small microvoids visible in Figure 7(b). The significant plasticity is not unexpected as the crack growth is occurring at a stress intensity approaching 90% of fracture toughness. In specimen 62B, less ductile fracture features are

visible within 100  $\mu\text{m}$  of the pre-crack (Figure 4) which is consistent with the stress intensity being lower during crack growth (72% of  $K_q$ ).

The results for the LT orientation (63B) indicate subcritical crack growth at the final two load steps of 5200 and 5600 lbs. Therefore, the  $K_{EAC}$  value indicated for the modified RSL protocol is equal to 39.0  $\text{ksi}\sqrt{\text{in}}$ , which is equal to 95% of the measured fracture toughness in air. The subcritical crack growth rates are similar to those obtained in for the ST orientation, namely,  $1.1 \times 10^{-4}$  to  $1.3 \times 10^{-4}$  in/hr.

## Summary

Test results are summarized in Table 2. Based on these results, AA7085-T7452 tested in the ST orientation shows EAC growth at a stress intensity as low as 72% of the fracture toughness. AA7085-T7452 tested in the LT orientation shows better performance with EAC growth at a stress intensity equal to 95% of the fracture toughness. Additional tests are warranted to firmly establish the lower bound of this value, as well as to quantify the statistical variability of  $K_{EAC}$ .

Table 2 - Summary of AA7085-T7452 test results.

Specimen	Environment	Loading Protocol	$K_q$ or $K_{EAC}$ ( $\text{ksi}\sqrt{\text{in}}$ )	Test time prior to EAC cracking (h)
62A (ST)	Air	0.01 in/min	27.9	NA
62B (ST)	ASTM seawater	400 lbs/16 holds	20.2	96
62C (ST)	ASTM seawater	2400 lbs + 400lbs/42h holds	25.2	126
63A (LT)	Air	0.01 in/min	41.2	NA
63B (LT)	ASTM seawater	2400 lbs + 400lbs/42h holds	39.0	294

## Notes

- Intergranular corrosion fissures were noted on the ST specimen fatigue pre-crack fracture surface due to solution exposure. The long axis of the fissures was parallel to the L direction of the specimen (Figure 4).
- Employing the requirement that  $K_{EAC}$  is 90% of  $K_q$  may be difficult for this material as the 10% of the fracture toughness corresponds to a mere 3  $\text{ksi}\sqrt{\text{in}}$ . The statistical variation of  $K_q$  should be established to confirm that a material is not disqualified due to an inherent variability in  $K_q$  measurement.

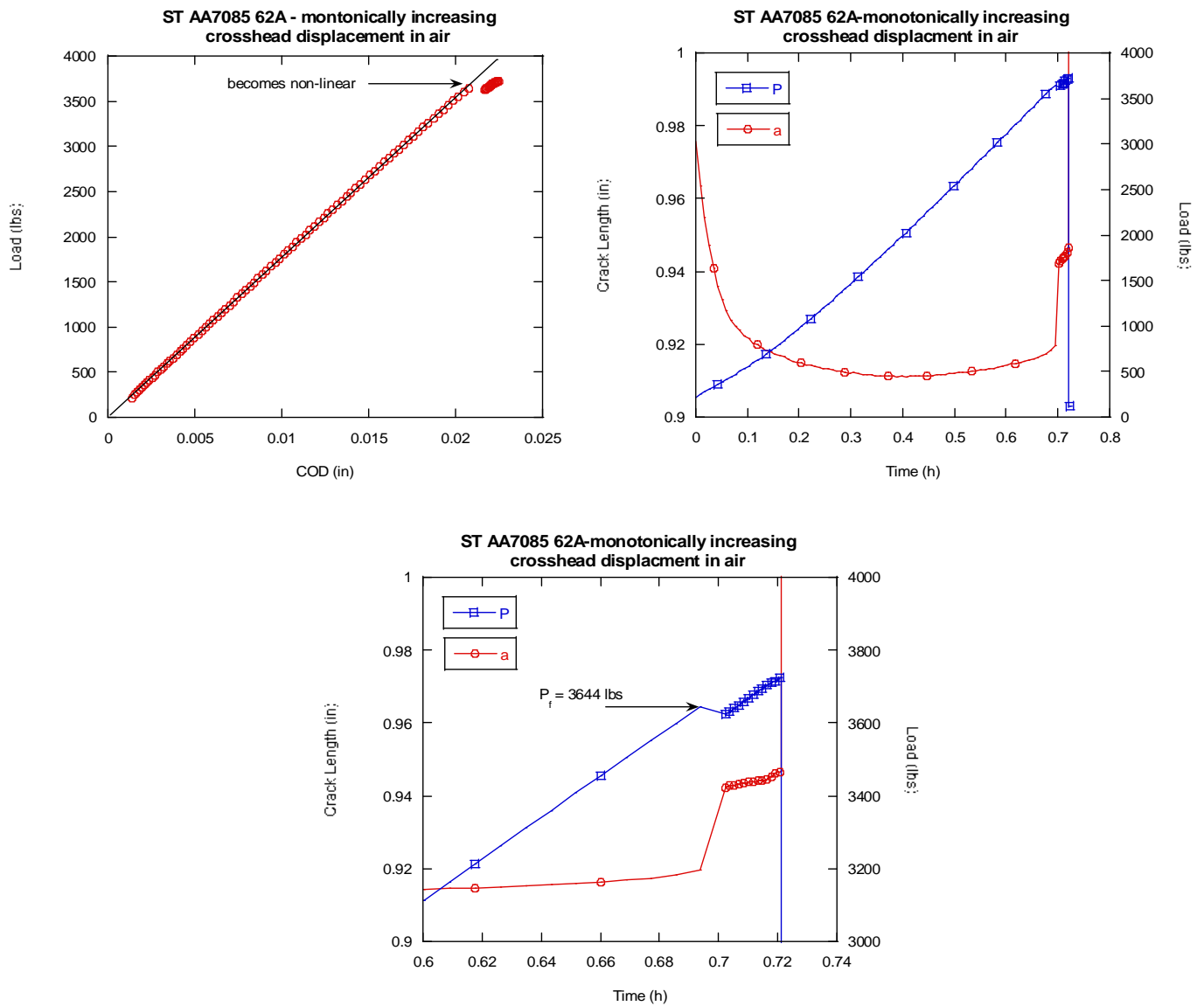
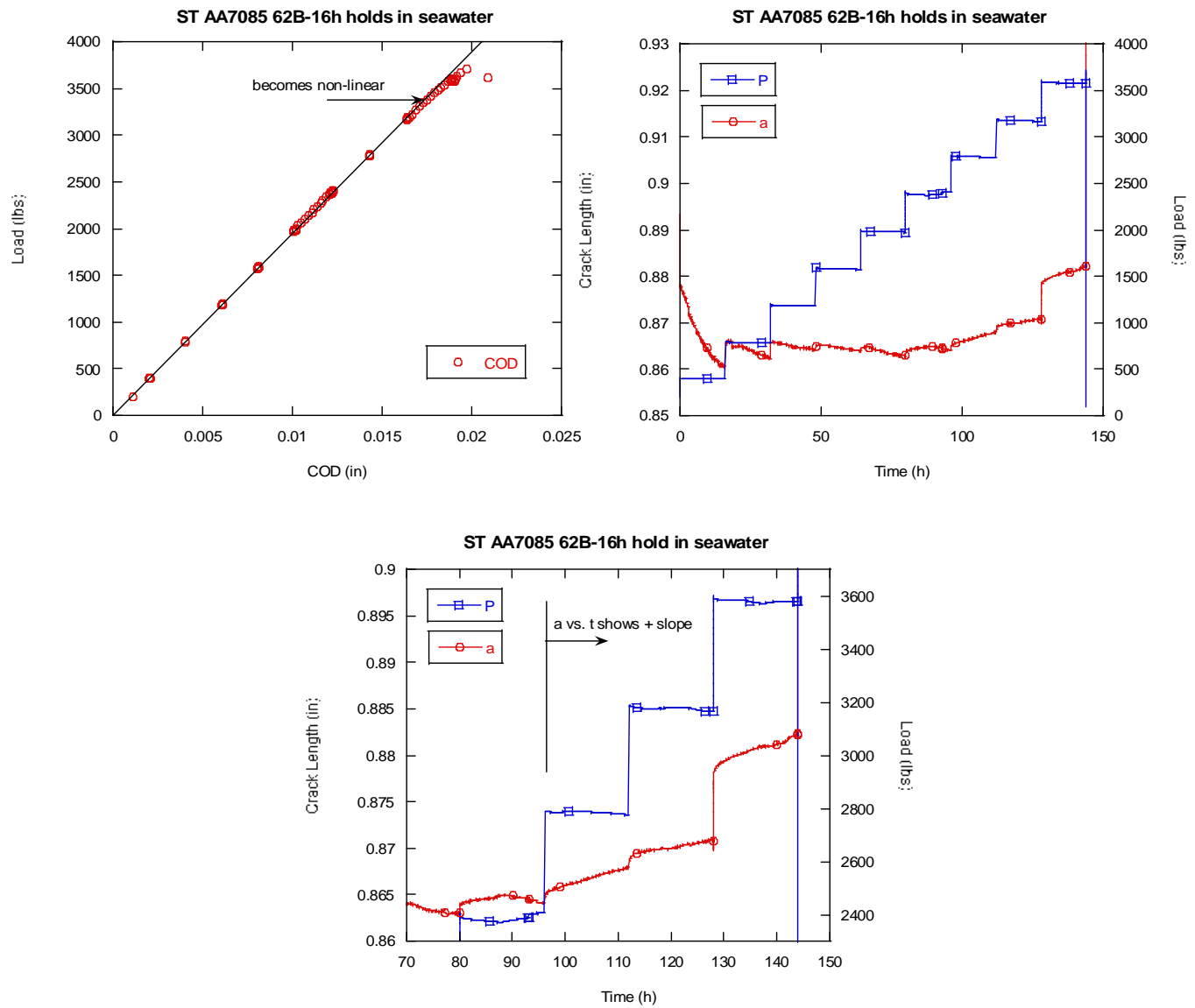
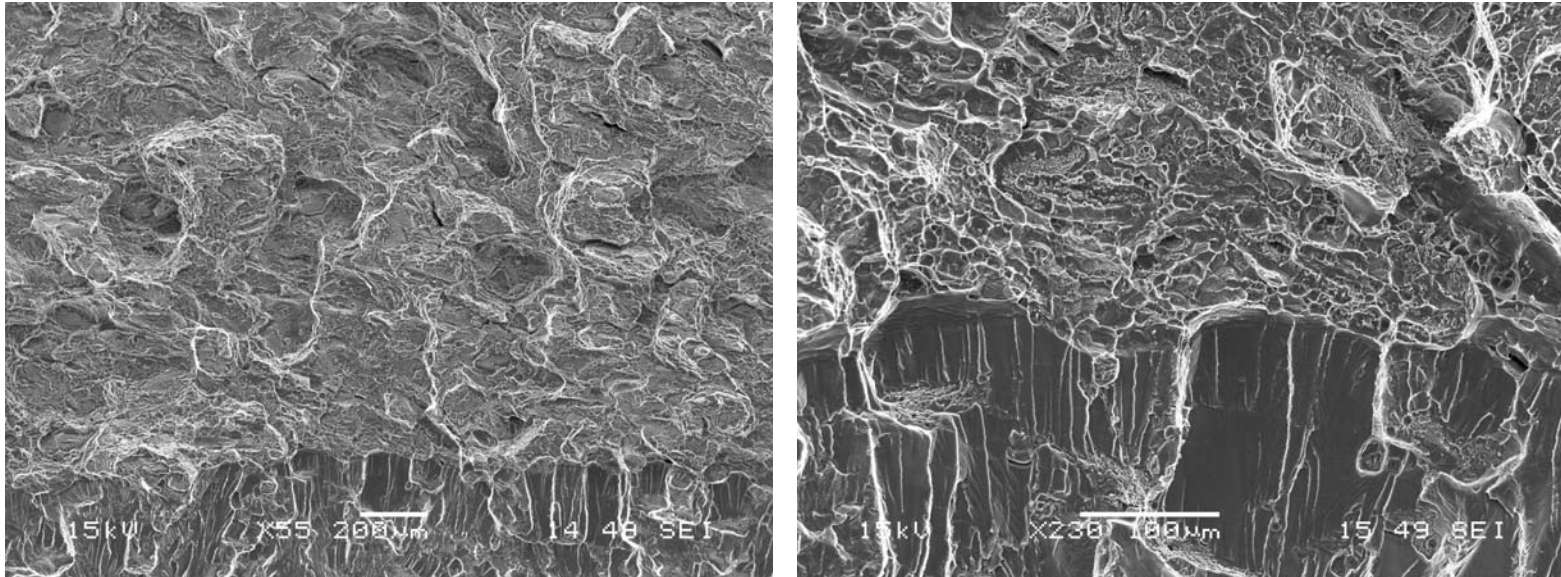


Figure 1 - Test results for ST specimen 62A that was tested in air at a monotonically increasing crosshead displacement.



**Figure 2 - Test results for ST specimen 62B that was tested in ASTM seawater using a rising step load protocol of 400 lb increases every 16 hours.**



**Figure 3 - SEM fractographs showing the fatigue pre-crack /fracture interface for ST specimen 62A tested in air. The fatigue pre-crack fracture surface is located at the bottom of the photo.**

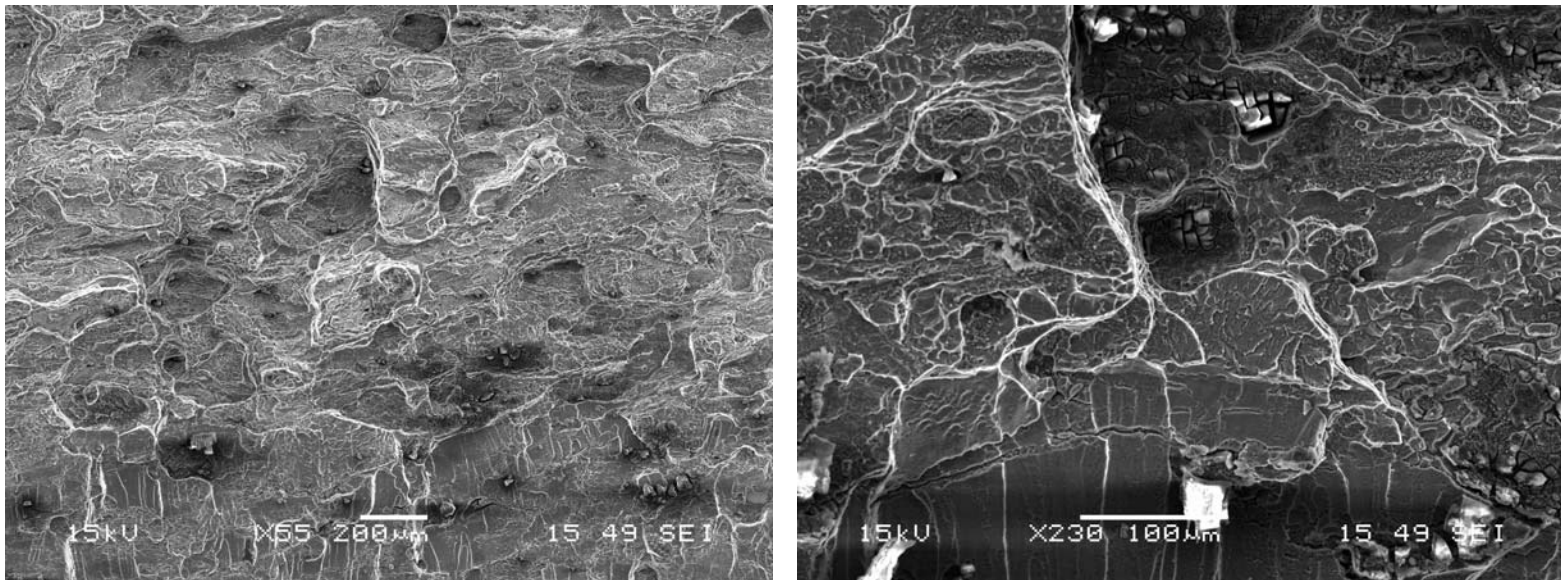


**Figure 4 - SEM fractographs showing the fatigue pre-crack /fracture interface for ST specimen 62B tested in seawater. The fatigue pre-crack fracture surface is located at the bottom of the photo.**

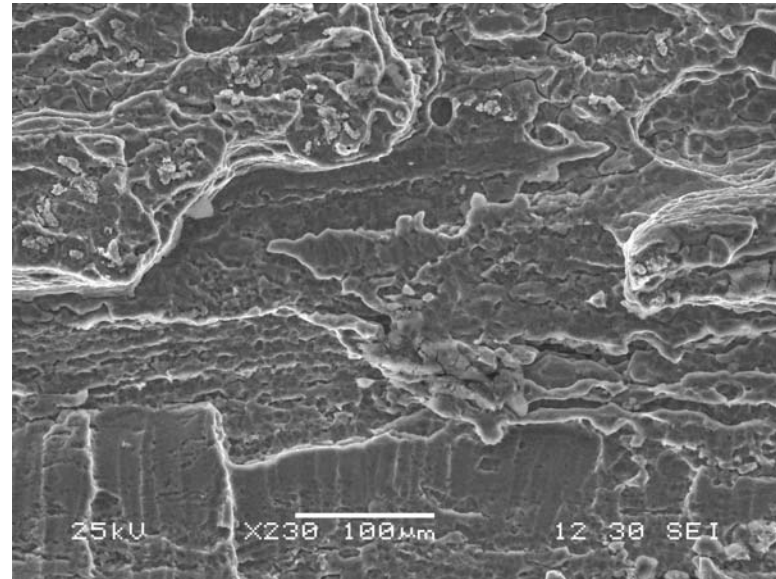
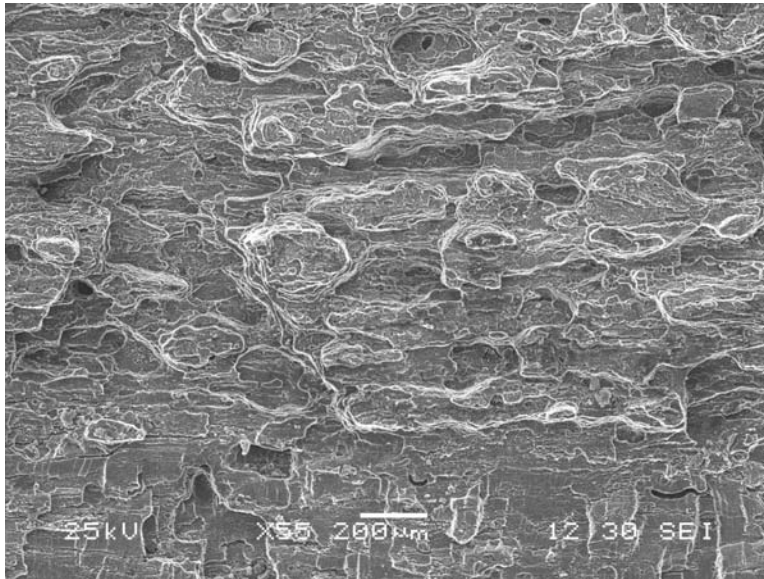


**Figure 6 - SEM fractographs showing the fatigue pre-crack /fracture interface for ST specimen 62C tested in seawater. The fatigue pre-crack fracture surface is located at the bottom of the photos.**

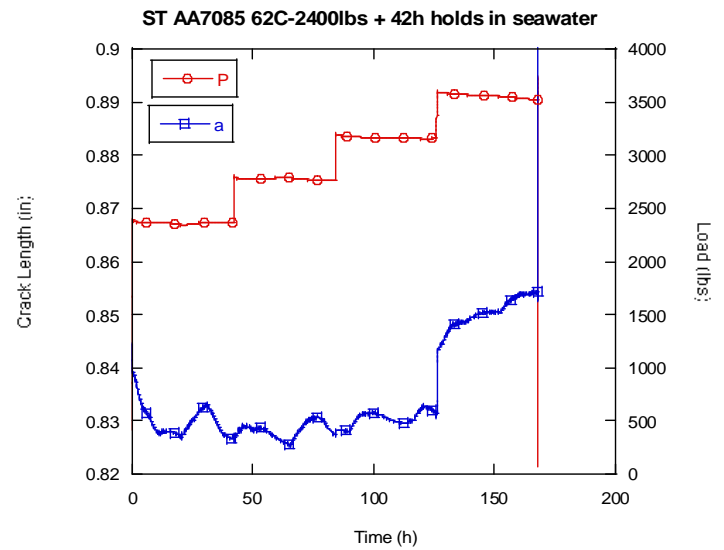
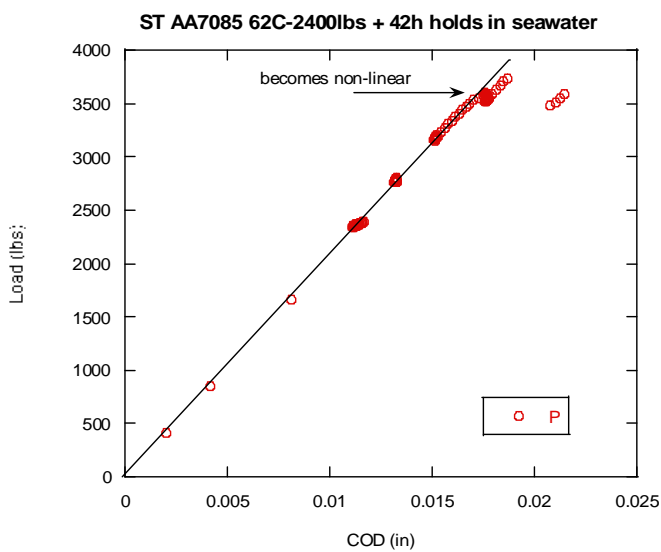


**Figure 5 - Test results for ST specimen 62C that was tested using a modified rising step load protocol, loading to 2400 lbs initially, followed by 400lb increases in load every 42 hours.**



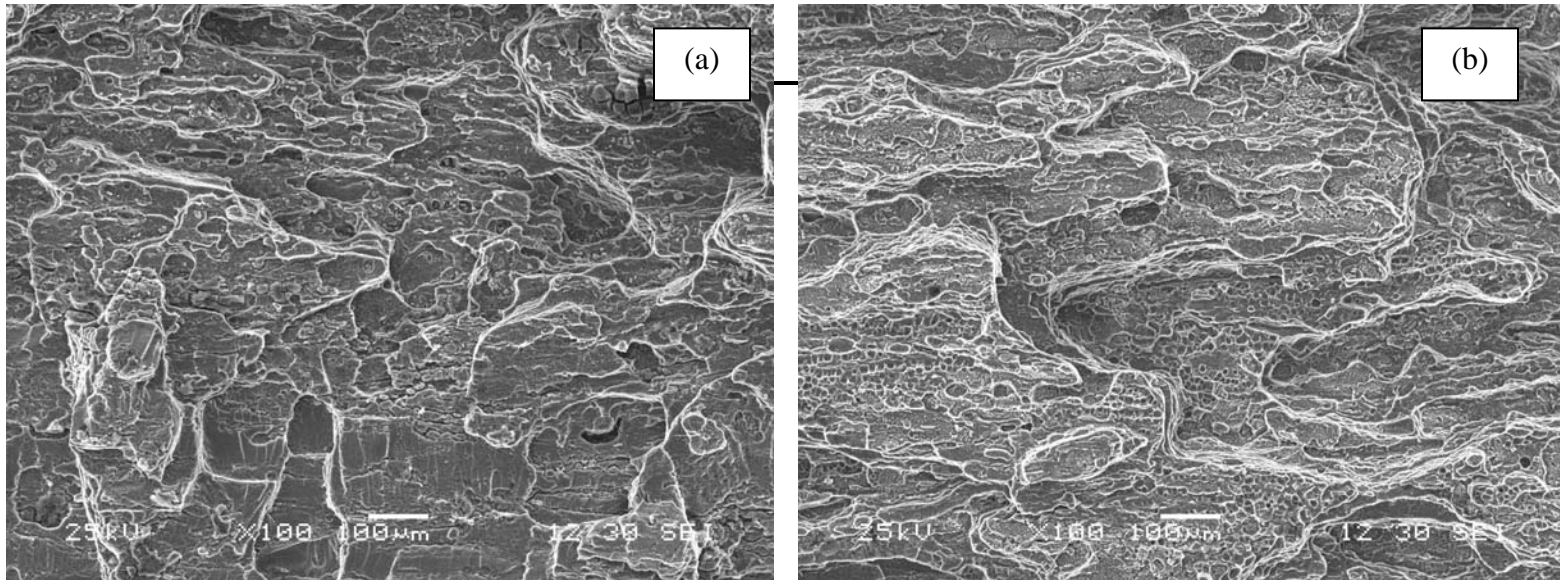


**Figure 7 - SEM fractographs of specimen ST 62C tested in seawater showing (a) the fracture surface near the fatigue pre-crack (located at the bottom of the photo) and (b) the fast fracture area well away from the pre-crack.**